J Mater Sci: Mater Med (2011) 22:515–523
DOI 10.1007/s10856-011-4236-4

Freeze extrusion fabrication of 13–93 bioactive glass scaffolds for bone repair

Nikhil D. Doiphode · Tieshu Huang · Ming C. Leu · Mohamed N. Rahaman · Delbert E. Day

Received: 26 August 2010 / Accepted: 12 January 2011 / Published online: 30 January 2011

Abstract A solid freeform fabrication technique, freeze extrusion fabrication (FEF), was investigated for the creation of three-dimensional bioactive glass (13–93) scaffolds with pre-designed porosity and pore architecture. An aqueous mixture of bioactive glass particles and polymeric additives with a paste-like consistency was extruded through a narrow nozzle, and deposited layer-by-layer in a cold environment according to a computer-aided design (CAD) file. Following sublimation of the ice in a freeze dryer, the construct was heated according to a controlled schedule to burn out the polymeric additives (below ~500°C), and to densify the glass phase at higher temperature (1 h at 700°C). The sintered scaffolds had a grid-like microstructure of interconnected pores, with a porosity of ~50%, pore width of ~300 μm, and dense glass filaments (struts) with a diameter or width of ~300 μm. The scaffolds showed an elastic response during mechanical testing in compression, with an average compressive strength of 140 MPa and an elastic modulus of 5–6 GPa, comparable to the values for human cortical bone. These bioactive glass scaffolds created by the FEF method could have potential application in the repair of load-bearing bones.

N. D. Doiphode · M. C. Leu (✉)
Department of Mechanical and Aerospace Engineering, Missouri University of Science and Technology, Rolla, MO 65409, USA
e-mail: mleu@mst.edu

T. Huang · M. N. Rahaman · D. E. Day
Department of Materials Science and Engineering, Missouri University of Science and Technology, Rolla, MO 65409, USA

1 Introduction

With an improved lifestyle and increased life span, the aging population disproportionately suffers from weakened bones and bone diseases. Bone diseases such as osteoporosis decrease the rate of bone remodeling, making weak bones prone to failure even during minor accidents. Current treatment methods such as bone autografts and allografts suffer from limitations, such as limited supply, danger of inflammatory response, and disease transfer. Metal implants are a substitute for natural grafts since they can be sterilized to avoid infection risk, and can be manufactured in sufficient quantity.

Metal implants bear a significant portion of working stresses and stop the natural process of bone remodeling by destroying its stimulus [1]. Mismatch between the stiffness of a metal graft and natural bone presents a danger of dislocation from surrounding bone under bending loads [2]. Metal implants often require replacement surgery after 15–20 years and some studies have cited their early failure [3]. Moreover, 'pseudotumours' due to the accumulation of soft tissue mass have been reported at the metal-hip resurfacing site [4]. With approximately 4 million implants expected by 2025 in the USA alone, the limitations of metal grafts for repairing bone defects provide a strong need for an alternative solution.

Tissue engineering can provide a better solution to this problem by regenerating natural bone using a surgically implanted porous, three-dimensional (3D) scaffold at the defect site [5]. With the advent of biologically active materials, scaffold materials are no longer restricted to function with only a minimal immune response but they are also designed to create a suitable environment for tissue growth [6–9].

Scaffold materials to be implanted in the human body are required to be biocompatible for minimal immune

reaction. Metals find very limited use in tissue engineering because of their bioinert nature. Natural polymers such as collagen, chitosan, hyaluronic acid, and alginate provide minimal problems with toxicity and inflammatory reactions, but variability in their properties and the need for room temperature fabrication can be limitations. The use of natural polymers and biodegradable synthetic polymers such as poly(glycolic acid), poly(lactic acid), poly(lactic co-glycolic acid), and polycaprolactone is limited to keeping minimum immune response [10, 11], but they lack bioactive properties for enhanced tissue growth.

Bioactive materials produce specific reactions when placed in contact with the body fluids and in the presence of suitable environmental conditions, leading to the formation of a hydroxyapatite-like surface layer that bonds strongly with bone and soft tissues [12, 13]. Hydroxyapatite (HA), synthetic or natural, is a widely studied bioactive material because of its osteoconductive nature. Third-generation bioactive materials, such as bioactive glass, are osteoconductive as well as osteoinductive. The silicate bioactive glass designated 45S5 has been reported to activate various families of genes through the release of Si, Ca, P and Na ions during its conversion to a HA-like material [12]. This gene activation is responsible for the upregulation of signaling factors which ultimately control the production of cell binding proteins, collagen, osteoblast cell cycle, and controlled cell apoptosis. The use of bioactive glass leads not only to the formation of a strong bond with the host bone but also to the stimulation of local tissue repair required for bone regeneration through rapid differentiation and proliferation of osteoblasts. Based on these advantages, bioactive materials and, in particular, bioactive glass are attractive candidate scaffold materials for bone repair.

While the most common method of producing a glass is melting and casting, this method cannot normally be used for the creation of 3D scaffolds because it provides very limited control of the pore architecture. Fabrication methods commonly used for the creation of bioactive glass scaffolds often use particles as starting materials, which are formed into the desired geometry and heated (sintered) to bond the particles into a strong glass network and interconnected pores. These methods include sintering of particles or short fibers, polymer foam replication, freeze drying, and phase separation. Polymer foam replication has been successfully used to fabricate scaffolds with a microstructure and strength similar to human trabecular bone [14], while unidirectional freezing of bioactive glass suspensions has been used to create scaffolds with oriented pores [15]. Other processing methods include sol–gel processing [16], solvent casting and particulate leaching [17], thermally induced phase separation, and micro-sphere sintering [18].

Solid freeform fabrication (or additive manufacturing) methods provide better control of the scaffold architecture than conventional methods. They have the potential for creating mechanically strong scaffolds with reproducible properties by improved control of the scaffold microstructure, such as porosity, pore size, pore size distribution, and pore orientation. Freeze extrusion fabrication (FEF) is an additive manufacturing process in which a paste is extruded through a narrow orifice and deposited layer-by-layer according to a designed computer-aided design (CAD) model. Freezing the deposited filaments in a cold environment reduces the tendency for distortion and slumping of the structure. FEF typically uses aqueous pastes and small quantities of organic binder (<5–10 vol%).

The objective of the present study was to investigate the use of FEF for the creation of 3D scaffolds of silicate 13–93 bioactive glass with a pre-designed porosity and pore architecture for potential bone repair applications. This bioactive glass was selected because products of this glass are approved for in vivo use in the US, Europe, and elsewhere. The major focus areas of this work were the development of an extrudable paste for the FEF method, determination of the FEF process variables, microstructural characterization of the fabricated scaffolds, and mechanical evaluation of the scaffolds.

2 Experimental procedure

2.1 FEF equipment

The FEF equipment consists of three subsystems (Fig. 1). A 3D gantry system facilitates the movement of a ram extrusion mechanism. Motion of the ram extruder is facilitated in the *X*, *Y* and *Z* directions using Velmax BiSlide orthogonal linear slides each with 250 mm travel. Two slides (in the *X*-axis) working in a master–slave fashion form the base of the fabrication setup. It supports the weight of the complete ram extruder assembly. The *Y*-axis slide is mounted on the two *X*-direction slides. The ram extruder assembly (in the *Z*-axis) is mounted on the *Y*-axis. All four slides are powered by Pacific Scientific PMA22B motors with 2.54 μm resolution for position feedback. Motion of the ram extruder is controlled by a delta-tau turbo programmable multi-axis controller. Ram movement is facilitated by a Kollmorgen AKM23D DC motor with a resolution of 0.254 μm, while the ram force during extrusion is measured by an Omega LC305-1KA load cell with a resolution of 2.2 N. The force signal (limited to ±250 mV) is sent to a delta-tau ACC28 board for feedback control of the extrusion process to provide a constant force of extrusion.

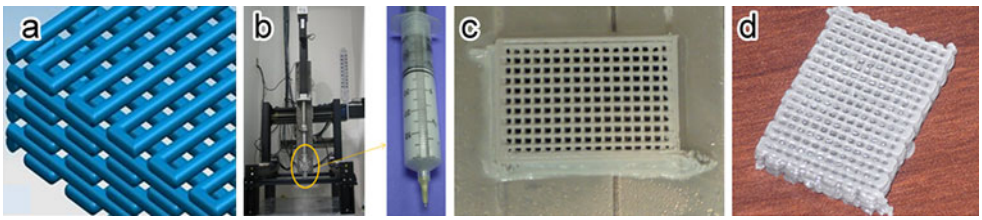

Fig. 1 Steps in the creation of a bioactive glass scaffold with a predesigned, grid-like microstructure by freeze extrusion fabrication (*FEF*): (**a**) computer-aided design (*CAD*) model of the part to be built; (**b**) photograph of gantry system and syringe in FEF machine; (**c**) as-formed part; (**d**) scaffold after post-processing steps (freeze drying, binder burnout, and sintering)

The 3D gantry is housed in an enclosure with a temperature control system to allow freezing of the extruded structure. Liquid nitrogen assisted cooling is used to provide freezing temperatures within the enclosure, and an Omega CN 132 temperature controller maintains freezing temperatures down to −30°C. The paste holder consists of a stainless steel sleeve and a plastic syringe fitted with a twist-on hypodermic needle. The paste holder is enclosed in a heating sleeve with an Omega DP7002 temperature controller to prevent the paste from freezing in the syringe.

The extruder ram is connected to the syringe for forced extrusion of the paste. Hypodermic needles with 580 μm nozzles were used for all fabrication experiments in this work. The designed CAD model is sliced in layers, and each layer is deposited on the previous layer by moving up the nozzle by one layer thickness in the *Z*-direction. The process continues until the desired 'green part' is created (Fig. 1).

For the creation of scaffolds with controlled porosity, the scaffold geometry was designed using the NX5 modeling software. The CAD model was exported in STL format, and the software package 'Insight' was used to design the scaffold's internal architecture with desired dimensions, raster patterns and pore size. Pores were designed by specifying the angle between two successive layers as 90° for all fabricated scaffolds. Pore size was varied by varying the distance between two adjacent lines of deposition.

2.2 Preparation of 13–93 bioactive glass paste

The bioactive glass (13–93) was kindly provided by Mo-Sci Health Care LLC, Rolla, Missouri. The as-received glass, prepared by conventional melting and casting, was crushed using a SPEX SamplePrep crusher (Model 8500, Metuchen, NJ), and attrition milled for 2.5 h using de-ionized water and ZrO_2 grinding media. The particle size distribution of the attrition milled glass was measured using a laser diffraction-based particle size analyzer (Model LS 13 320; Beckman Coulter Inc., Fullerton, CA). The attrition-milled slurry was dried and the dried glass powder was sieved through a 106 μm stainless steel sieve.

An extrudable paste for FEF was prepared as follows. First, a slurry was prepared by ball milling of a mixture of bioactive glass particles, de-ionized water, and appropriate quantities of polymeric additives (binder, dispersant, and surfactant) for 24 h using Al_2O_3 grinding media. The composition of the starting mixture is given in Table 1. Next, the ball-milled slurry was converted to a paste with the required viscosity by heating the slurry for 70 min at 65°C to evaporate some liquid (weight loss = 4%). The paste was vacuum mixed for 30–45 s (WhipMix Vacuum Power Mixer Plus; WhipMix Corporation, Louisville, KY), and transferred to a 60 cc plastic syringe. Extrusion trials were carried out using the paste of this composition to determine if it could be used to fabricate different profiles requiring extrusion on demand (i.e., start and stop of extrusion as desired). The extrusion process was observed for paste consistency and the amount of binder was increased in the subsequent compositions to achieve uniform filaments of material. The extrusion force was determined experimentally by observing the nature of the extrudate at different forces.

The paste composition and extrusion force which showed consistent extrusion were used for multilayered scaffold fabrication. Paste discharge through the nozzle was measured for steady-state extrusion and the viscosity η was determined using the equation:

$$\eta = \frac{\pi R^4 P}{8LQ} \quad (1)$$

where R is the nozzle diameter (2 mm), L is the length of the nozzle opening (20 mm), Q is the discharge rate (mm^3/s) and P is the extrusion pressure (Pa). The paste viscosity was measured as a function of extrusion force in order to study the paste behavior at different extrusion forces.

2.3 Post-processing of as-formed FEF part

The as-formed FEF article was freeze dried to sublime the ice, then heated to burn out the polymer additives and to

Table 1 Composition of starting slurry used in the preparation of the extrudable paste for freeze extrusion fabrication

Component	Concentration (vol%)	Function	Manufacturer
13–93 Glass particles	40.00	Solid phase	Mo-Sci Corp., Rolla, MO
EasySperse	0.50	Dispersant	ISP Technologies, Inc., Wayne, NJ
Surfnol	0.50	Defoamer	Air Products & Chemicals, Inc., Allentown, PA
Glycerol	1.00	WCCA	Alfa Aesar, Ward Hill, MA
PEG 400	1.00	Lubricant	Alfa Aesar, Ward Hill, MA
Aquazol 5	4.00	Binder	ISP Technologies, Inc., Wayne, NJ
Deionized water	53.00	Solvent	–

WCCA water crystallization control agent

Table 2 Binder burnout schedule used for the 13–93 bioactive glass scaffolds formed in this work by freeze extrusion fabrication

Starting temperature (°C)	Ending temperature (°C)	Heating rate (°C/min)	Hold period (h)
30	120	2	2
120	250	0.1	6
250	320	0.5	12
320	350	0.05	12
350	440	0.05	12
440	600	5	12

sinter the glass particles into a dense interconnecting network. The development of the binder burnout schedule (Table 2) was based on the thermogravimetric analysis (NETZSCH Model STA 409) of the bioactive glass paste at a heating rate of 2°C/min in air. After the binder burnout step, the constructs were sintered for 1 h at 700°C (heating rate = 5°C/min).

2.4 Characterization of bioactive glass scaffolds

Scanning electron microscopy, SEM (S-4700; Hitachi, Tokyo, Japan) was used to observe the microstructure and fractured cross-sections of the as-formed scaffolds and the sintered scaffolds. X-ray diffraction (XRD–Philips PAN-analytical X-Pert) was used to analyze for the presence of any crystalline phases in the starting bioactive glass particles and in the sintered scaffolds. XRD was performed using copper K_α radiation ($\lambda = 0.15406$ nm) at a scanning rate of 0.01° 2θ/min in the range 3–90°.

The compressive strength and elastic modulus of the sintered scaffolds were measured using an Instron testing machine (Model 4204; Instron Corp., Norwood, MA). Cube-shaped specimens (5 mm × 5 mm × 5 mm) were cut from the central portion of the sintered scaffolds (to minimize edge effects of the scaffolds) and tested at a deformation rate of 0.2 mm/min. Six samples were tested to determine a mean value ± standard deviation.

3 Results

Figure 2a shows the size distribution of the attrition milled bioactive glass particles used in this work. The particle size varied from ~0.4 to ~15 μm, with a mass median diameter, D_{50}, of 2.1 μm. SEM showed that the particles had an angular shape, typical of brittle particles prepared by milling (Fig. 2b).

Extrusion trials of the initial bioactive glass paste composition through the FEF syringe did not show uniform and consistent extrusion. Frequent curling of the extrudate and clogging of the nozzle were frequently observed. By increasing the binder content of the paste (Aquazol 50), and adding a plasticizer, poly(ethylene glycol), and glycerol to prevent the formation of ice during the extrusion, consistent extrusion of filaments was achieved. Figure 3 shows examples of non-consistent, non-uniform extrusion with the initial paste composition, and significantly improved extrusion with the modified composition. Henceforth, the modified paste composition given in Table 1 was used.

The change in paste viscosity with extrusion force is shown in Fig. 4. The data show an initial increase in viscosity with increasing extrusion force, presumable caused by the removal of excess liquid at the beginning of the extrusion. It was found necessary to remove the excess liquid before each scaffold fabrication run. The pores in the scaffold were fabricated by specifying gaps between the adjacent paths of the filaments and alternating the direction of deposition for successive layers. If the initial free extrusion was not carried out to remove the excess liquid, the gaps between the adjacent paths were not maintained, resulting in a solid structure with inaccurate fabrication. Figure 5 illustrates the difference in the first layer deposition before and after removal of the excess liquid. Following the initial increase, there was a decrease in the paste viscosity with increasing extrusion force (Fig. 4). Paste flow through the nozzle was facilitated by lower viscosity as a result of higher shear stresses due to extrusion force. The presence of a plasticizer (PEG-400) also

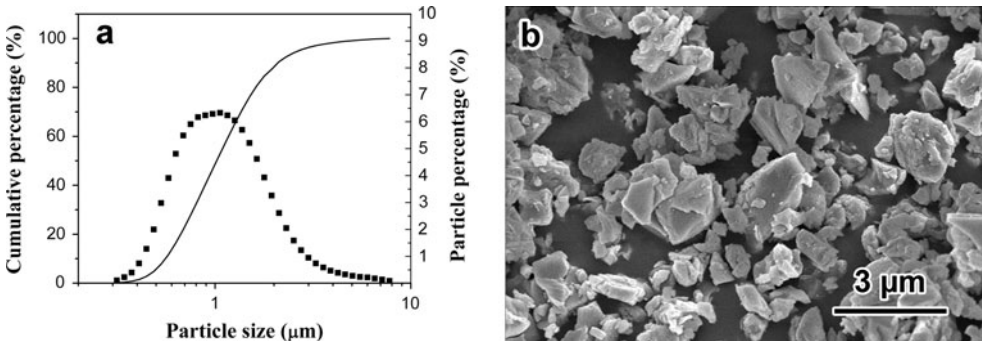

Fig. 2 (**a**) Particle size distribution of 13–93 glass used in the formation of the extrudable paste; (**b**) SEM image of the particles

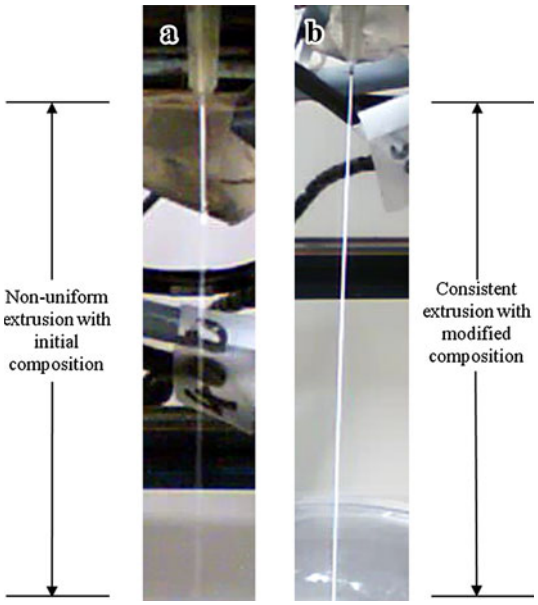

Fig. 3 Examples of extruded filaments in FEF: (**a**) starting paste showing non-uniform extrusion; (**b**) optimized paste with consistent extrusion

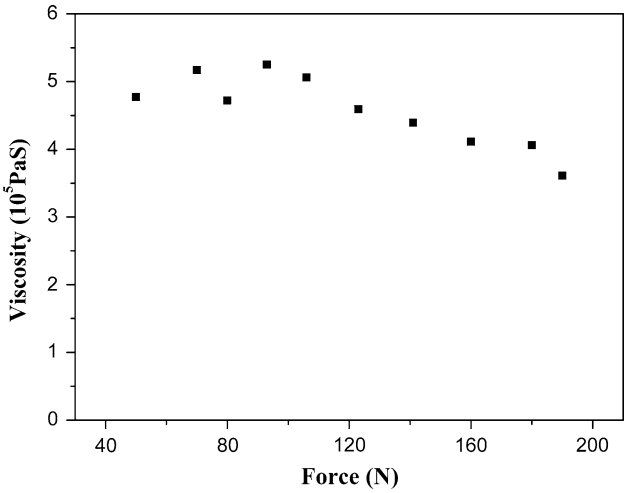

Fig. 4 Dependence of paste viscosity on extrusion force

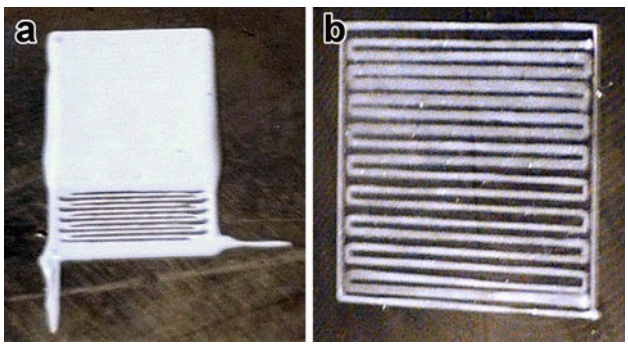

Fig. 5 Effect of removing excess liquid from the paste prior to deposition of first layer: (**a**) without removal of excess liquid; (**b**) after removal of excess liquid

improved the flow behavior of the paste. For robotic deposition of thick pastes, it is well established that the paste must flow smoothly through the deposition nozzle and retain its shape after deposition on the work table [19–23]. With the viscosity changes described, the modified composition facilitated smooth flow through the nozzle and also maintained the shape of the deposited profile.

Layer-by-layer scaffold fabrication was started after achieving steady state extrusion. Environmental temperature was varied between –7 and –22°C depending on the pore size in the scaffold. For smaller pores, gaps between the adjacent paths were maintained with the help of lower environmental temperature (–15 to –22°C). The nozzle tip was cleaned after depositing every layer to ensure unobstructed flow of paste, and the extrusion force used was in the range of 200–250 N. Figure 6 shows an example of a bioactive glass 'green scaffold' fabricated with a pore size (width) of 600 μm. The scaffold dimension was 36 mm × 30 mm × 6 mm. Similar scaffolds with pore widths of 800 μm of 1,000 μm were fabricated by increasing the distance between the adjacent filaments.

Figure 7 shows a thermogravimetric curve (weight vs. temperature) for the decomposition of the bioactive glass paste. Noticeable changes in the slope of the curve appeared to occur at approximately 80, 240, 320, 350 and 440°C. The low melting point polymers and residual water are evaporated in the temperature range 80–120°C, glycerol is evaporated in the range ~120–170°C, and the

higher molecular weight polymers from ~170–600°C. Table 2 summarizes the binder burnout schedule used for the scaffolds.

Figure 8 shows a sintered scaffold and its cross-section (in the thickness direction). The average shrinkage in the length, width and thickness of the scaffold was 28%, 24%, and 20%, respectively. Pores of width 600 μm in the green part (after formation by FEF) became ~500 μm after sintering, while pores of width 800 μm and 1,000 μm became ~700 μm and ~900 μm, respectively, after sintering. SEM images of the fractured cross-sections of the green part and the sintered scaffold show that the glass particles in the green part appeared to have a high packing density (Fig. 9a, b), while the glass filaments in each layer of the sintered scaffold were almost fully dense, with only a few isolated pores (*arrow*), and well bonded to the filaments in the adjacent layers (Fig. 9c).

The XRD pattern of the sintered glass scaffold was similar to that of the starting glass particles (Fig. 10), consisting of a broad band at ~30° 2θ, typical of an amorphous glass [14]. This indicates that the amorphous nature of the bioactive glass was maintained during the binder burnout and sintering steps, with no observable crystallization of the glass. For the six samples of the sintered scaffolds tested, the compressive strength was 140 ± 70 MPa.

4 Discussion

The results of the present work showed the ability of the FEF process for creating 13–93 bioactive glass scaffolds with a predesigned grid-like microstructure, consisting of dense glass filaments and interconnected pores. The pore characteristics of the scaffolds (porosity = 50%; pore width 300 μm) are known to be capable of supporting tissue ingrowth, while the average compressive strength (140 MPa) is in the range of values reported for human cortical bone (100–150 MPa).

The high compressive strength obtained with these 13–93 bioactive glass scaffolds created by FEF can be attributed to the ability to achieve a dense glass phase with a uniform porous microstructure. The ability to achieve a dense glass phase can, in turn, be attributed to three main factors: (1) high packing density and homogeneous packing of the glass particles in the as-formed green part; (2) fine particle size of the glass powder, leading to a high driving force for viscous flow sintering; and (3) favorable viscous flow sintering characteristics of the 13–93 bioactive glass. Using aqueous pastes in FEF might provide an advantage over powder-based layer-by-layer manufacturing processes such as selective laser sintering. Structural integrity and strength in a layered additive manufacturing process depends on adhesion between successive layers. In FEF, an aqueous paste provides better mixing than partially wetting pastes or powders at the contact area between two successive layers. This provides a strong bond resisting delamination of the layers. Also, freezing the extruded filaments helps the deposited structure to maintain its shape. During the binder burnout and sintering, this contact is again strengthened. The scaffold has a well-defined structure of macro-pores. The interconnectivity of macro-pores (Fig. 9a) is maintained during the green part fabrication and the post processing. These macro-pores will allow exchange of nutrients and waste for effective tissue in-growth.

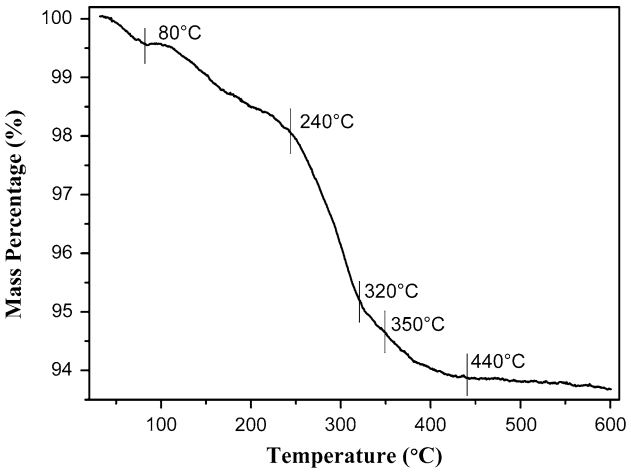

Fig. 7 Thermogravimetric analysis of paste used in FEF

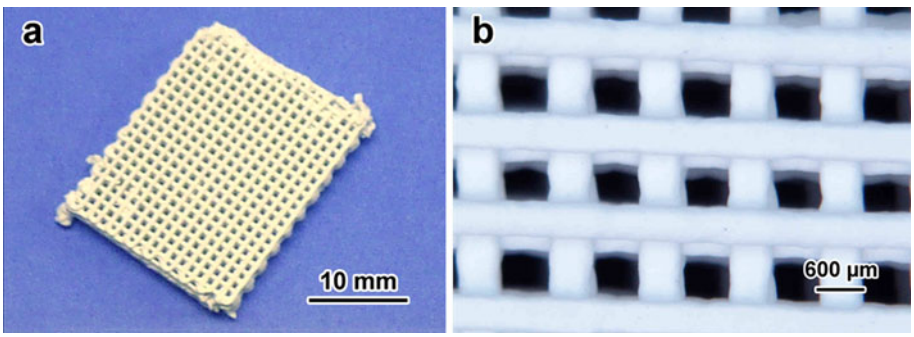

Fig. 6 Optical images of bioactive glass scaffold as formed by FEF. (**a**) Whole sample view and (**b**) magnified image shows the uniform structure

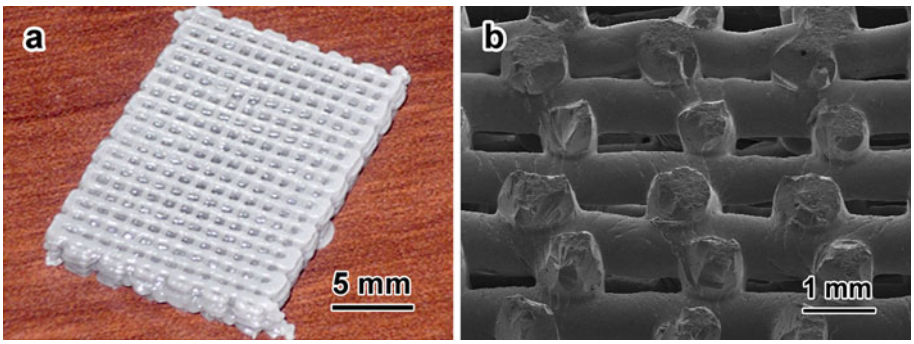

Fig. 8 (**a**) Optical image of sintered scaffold showing the retention of the shape after the post-processing steps; (**b**) SEM image of the fractured cross-section of the sintered scaffold showing good bonding between adjacent layers of the scaffold

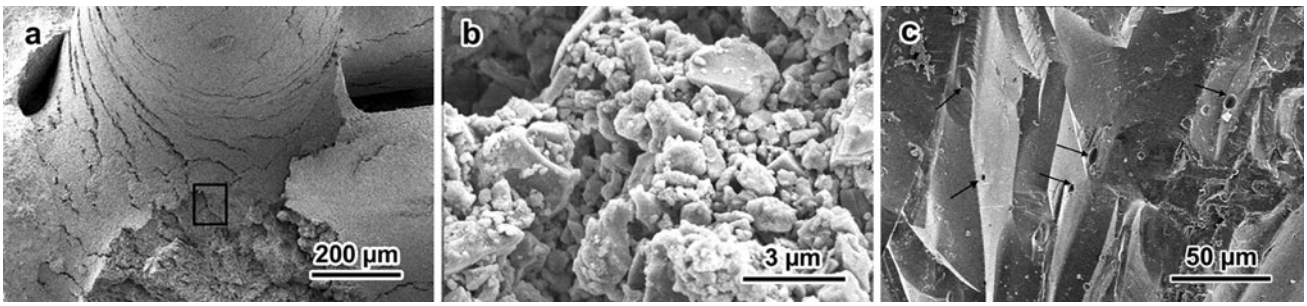

Fig. 9 SEM images of (**a**), (**b**) as-formed scaffold after deposition by FEF, showing good packing of the glass particles, and (**c**) the sintered scaffold showing that the glass struts were almost fully dense

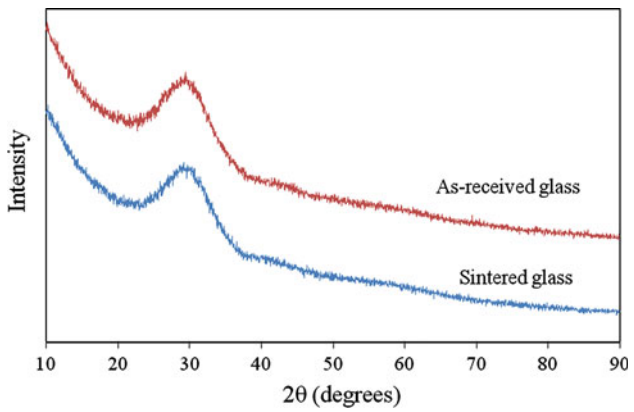

Fig. 10 X-ray analysis of starting 13–93 glass particles and sintered scaffold, showing no observable crystallization of the glass during the scaffold fabrication process

In FEF, freezing of the extruded filaments helps to control the spread of the paste on the work table. The paste is frozen as it is deposited thus providing a supporting base for successively deposited layers. Other strategies reported elsewhere to control the spread of paste on the work table include the use of a volatile solvent in the paste. In this case, the solvent is evaporated as the paste is deposited thereby creating a solid region around the deposited profile [24]. This method using the partial wetting of pastes is believed to provide bonding between successive layers and requiring less control over paste rheology [21]. With the aqueous based pastes in FEF, a more robust contact between the successive layers is obtained providing a better bonding between successive layers.

Scaffolds for bone tissue engineering are required to have open porosity of at least 50% [7, 9, 25–28]. While different studies indicate different values for the optimum pore size of the scaffold capable of supporting tissue ingrowth, it is widely accepted that the minimum pore size capable of supporting tissue ingrowth is 100–200 μm [7, 9, 25–28]. The ability to achieve the desired mechanical strength while maintaining the above requirements of porosity, pore size and pore interconnectivity is an important aspect of scaffold fabrication.

In other studies, oriented HA scaffolds with lamellar architecture (porosity 47%; pore size <50 μm), prepared by unidirectional freezing of suspensions, have shown average compressive strengths of 145 MPa in the orientation direction [29]. While the strength is comparable to that of cortical bone (100–150 MPa) [6, 30–32], the pore width of the scaffold (typically <50 μm) is considered to be too small to support tissue ingrowth. Extrusion-based robocasting has been used to fabricate HA scaffolds with 55% porosity and pore width of ~200 μm using partially wetting inks [33]. In that study, evaporation of the solvent (methylene chloride) was used as the consolidation mechanism between adjacent layers. The highest compressive strength achieved for HA scaffolds was ~22 MPa. The elastic modulus was reported to vary between 24 and 150 MPa with different polymer combinations and testing directions, which is far lower than the elastic modulus of

human cortical bone (5–15 GPa) [34]. Robocasting of partially flocculating suspensions of HA in an oil bath has been used to fabricate scaffolds (porosity = 40%; pore width ≈ 100 μm) with a compressive strength of ~50 MPa [23, 35]. Infiltration of the HA scaffolds in SBF resulted in an increase of the compressive strength to ~115 MPa [36].

Scaffolds of the bioactive glass designated 6P53B, prepared by robocasting of partially wetting inks [33], have shown a compressive strength of ~7 MPa and an elastic modulus of ~105 MPa (porosity = 75%; pore width ≈ 200 μm), which are much lower than the compressive strength and elastic modulus of human cortical bone. Bioactive glass (13–93) scaffolds with columnar microstructure (porosity = 55–60%; pore width = 90–100 μm), fabricated by unidirectional freezing of suspensions, have shown a compressive strength of 25 MPa [15]. Scaffolds fabricated by indirect selective laser sintering of bioactive glass particles have not shown compressive strengths higher than that of human trabecular bone [37–40].

The average compressive strength (140 MPa) obtained in this work for 13–93 bioactive glass scaffolds fabricated by FEF is comparable to the compressive strength of human cortical bone. This strength is also higher than the strengths reported in the literature for scaffolds fabricated by other manufacturing methods (additive or non-additive). Since 13–93 bioactive glass is already known to support new bone growth [14, 15, 41–44], these bioactive glass scaffolds fabricated using FEF have promising potential for use in the repair of load-bearing bones.

5 Conclusion

FEF was shown to be a viable method for the creation of porous, 3D bioactive glass (13–93) scaffolds with a compressive strength (140 ± 70 MPa) comparable to that of human cortical bone. An aqueous mixture of bioactive glass particles and polymeric additives with a paste-like consistency was developed for extrusion in the FEF process. The scaffold maintained its geometry and microstructure after extrusion and post processing (binder burnout; sintering). The fabricated scaffold, with a grid-like microstructure, consisted of almost fully dense glass struts and pore characteristics (porosity = 50%; pore width ≈ 300 μm) known to be capable of supporting tissue ingrowth. These bioactive glass scaffolds created by FEF could have potential application in the repair of load-bearing bones.

Acknowledgments The authors acknowledge the financial support for this research by the Center for Bone Tissue Repair and Regeneration at Missouri University of Science and Technology. The bioactive glass (13–93) used in this work was kindly provided by Mo-Sci Corp., Rolla, Missouri.

References

1. Wolff J. The law of bone remodeling, translated from the 1982 original Das Gesetz der Transformation der Knochen, by P. Maquet and R. Furlong. Springer Verlag: Berlin, Heidelberg, New York; 1986.
2. Woesz A. Rapid prototyping to produce porous scaffolds with controlled architecture for possible use in bone tissue engineering. In: Bidanda B, Bártolo P, editors. Virtual prototyping and bio manufacturing in medical applications. New York: Springer; 2008. p. 171–206.
3. Mikhael MM. Failure of metal-on-metal total hip arthroplasty mimicking hip infection. J Bone Joint Surg. 2009;91-A:443–6.
4. Pandit H, Glyn-jones S, McLardy-Smith P, Gundle R, Whitwell D, Gibbons CLM, Ostlere S, Athanasou N, Gill HS, Murray DW. Pseudotumours associated with metal-on-metal hip resurfacings. J Bone Joint Surg Br. 2008;90B:847–51.
5. Tsuruga E, Takita H, Itoh H, Wakisaka Y, Kuboki Y. Pore size of porous hydroxyapatite as the cell-substratum controls BMP-induced osteogenesis. J Biochem. 1997;121:317–24.
6. Rezwan K, Chen QZ, Blaker JJ, Boccaccinni AR. Biodegradable and bioactive porous polymer/inorganic composite scaffolds for bone tissue engineering. Biomaterials. 2006;27:3413–31.
7. Guarino V, Causa F, Ambrosio L. Bioactive scaffolds for bone and ligament tissue. Expert Rev Med Devices. 2007;4:405–18.
8. Ma PX. Scaffolds for tissue fabrication. Mater Today. 2004;7:30–40.
9. Chen Q, Roether JA, Boccaccinni AR. Tissue engineering scaffolds from bioactive glass and composite materials. Topics Tissue Eng. 2008;4:1–27.
10. Bergsma EJ, Rozema FR, Bos RRM, Debruijn WC. Foreign body reaction to resorbable poly(L-lactide) bone plates and screws used for the fixation of unstable zygomatic fractures. J Oral Maxillofac Surg. 1993;51:666–70.
11. Martin C, Winet H, Bao JY. Acidity near eroding polylactide–polyglycolide in vitro and in vivo in rabbit tibia bone chambers. Biomaterials. 1996;17:2373–80.
12. Hench LL, Polak JM, Buttery Lee DK, Xynos ID, Maroothynaden J. Use of bioactive glass composites to stimulate osteoblast production. US Patent No. 0009598A1; Jan 2004
13. Hench LL, Polak JM. Third-generation biomaterials. Science. 2002;295:1014–7.
14. Fu Q, Rahaman MN, Bal SB, Brown RF, Day DE. Mechanical and in vitro performance of 13–93 bioglass scaffolds prepared by polymer foam replication technique. Acta Biomater. 2008;4:1854–64.
15. Fu Q, Rahaman MN, Bal SB, Brown RF. Preparation and in vitro evaluation of bioactive glass (13–93) scaffolds with oriented microstructures for repair and regeneration of load-bearing bones. J Biomed Mater Res Part A. 2010;93A:1380–90.
16. Sepulveda P, Jones JR, Hench LL. Bioactive sol–gel foams for tissue repair. J Biomed Mater Res. 2002;59:340–8.
17. Ma PX, Choi JW. Biodegradable polymer scaffolds with well-defined interconnected spherical pore network. Tissue Eng. 2001;7:23–33.
18. Lu HH, El-Amin SF, Scott KD, Laurencin CT. Three dimensional, bioactive, biodegradable, polymer-bioactive glass composite scaffolds with improved mechanical properties support collagen synthesis and mineralization of human osteoblast-like cells in vitro. J Biomed Mater Res Part A. 2003;64:465–74.

19. Cesarano J, Calvert PD. Freeforming objects with low-binder slurry. US Patent Number 6027326; Feb 2000
20. Smay JE, Gratson GM, Shepherd RF, Cesarano J, Lewis JA. Directed colloidal assembly of 3D periodic structures. Adv Mater. 2002;14:1279–83.
21. Smay JE, Cesarano J, Lewis JA. Colloidal inks for directed assembly of 3D periodic structures. Langmuir. 2002;18:5429–37.
22. Michna S, Willie W, Lewis JA. Concentrated hydroxyapatite inks for direct-write assembly of 3-D periodic scaffolds. Biomaterials. 2005;26:5632–9.
23. Miranda P, Saiz E, Gryn K, Tomsia AP. Sintering and robocasting of β-tricalcium phosphate scaffolds for orthopedic applications. Acta Biomater. 2006;2:457–66.
24. Russias J, Saiz E, Deville S, Gryn K, Liu G, Nalla RK, Tomsia AP. Fabrication and in vitro characterization of three-dimensional organic/inorganic scaffolds by robocasting. J Biomed Mater Res Part A. 2007;83A:434–45.
25. Hollinger JO, Leong K. Poly(alpha-hydroxy acids): carriers for bone morphogenetic proteins. Biomaterials. 1996;17:187–94.
26. Hu YH, Grainger DW, Winn SR, Hollinger JO. Fabrication of poly(-hydroxy acid) foam scaffolds using multiple solvent systems. J Biomed Mater Res. 2002;59:563–72.
27. Hutmacher DW. Scaffolds in tissue engineering bone and cartilage. Biomaterials. 2000;21:2529–43.
28. Burg KJL, Porter S, Kellam JF. Biomaterial developments for bone tissue engineering. Biomaterials. 2000;21:2347–59.
29. Deville S, Saiz E, Tomsia AP. Freeze casting of hydroxyapatite scaffolds for bone tissue engineering. Biomaterials. 2006;27:5480–9.
30. Fung YC. Biomechanics mechanical properties of living tissues. New York: Springer; 1993. p. 500.
31. Keaveny TM, Hayes WC. Mechanical properties of cortical bone and trabecular bone. In: Hall BK, editor. Bone growth. Boca Racon, FL: CRC press; 1993. p. 285–344.
32. Rho J-Y. Mechanical properties and the hierarchical structure of bone. Med Eng Phys. 1998;20:92–102.
33. Russias J, Saiz E, Deville S, Gryn K, Liu G, Nalla RK, Tomsia AP. Fabrication and in vitro characterization of three-dimensional organic/inorganic scaffolds by robocasting. J Biomed Mater Res Part A. 2007;83A:434–45.
34. Cowin SC. Bone mechanics handbook. 2nd ed. London UK: Informa Healthcare; 2001. p. 101–1023.
35. Miranda P, Pajares A, Saiz E, Tomsia AP, Guiberteau F. Fracture modes under uniaxial compression in hydroxyapatite scaffolds fabricated by robocasting. J Biomed Mater Res, Part B Appl Biomater. 2007;83A:646–55.
36. Miranda P, Pajares A, Saiz E, Tomsia AP, Guiberteau F. Mechanical properties of calcium phosphate scaffolds fabricated by robocasting. J Biomed Mater Res Part A. 2008;85A:218–27.
37. Lorrison JC, Goodridge RD, Dalgarno KW, Wood DJ. Selective laser sintering of bioactive glass-ceramics, Solid Freeform Fabrication Proceedings. University of Texas at Austin; 2002, pp. 1–8
38. Lorrison JC, Dalgarno KW, Wood DJ. Processing of an apatite-mullite glass-ceramic and an hydroxyapatite/phosphate glass composite by selective laser sintering. J Mater Sci Mater Med. 2005;16:775–81.
39. Goodridge RD, Dalgarno KW, Wood DJ. Indirect selective laser sintering of an apatite-mullite glass-ceramic for potential use in bone replacement applications. PhD thesis, University of Leeds, UK; 2005
40. Roodridgee RD, Wood DJ, Ohtsuki C, Dalgarno KW. Biological evaluation of an apatite-mullite glass-ceramic produced via selective laser sintering. Acta Biomater. 2006;3:221–31.
41. Fu Q, Rahaman MN, Day DE. Accelerated conversion of silicate bioactive glass (13–93) to hydroxyapatite in aqueous phosphate solution containing polyanions. J Am Ceram Soc. 2009;92:2870–6.
42. Brown RF, Day DE, Day TE, Jung S, Rahaman MN, Fu Q. Growth and differentiation of osteoblastic cells on 13–93 bioactive glass fibers and scaffolds. Acta Biomater. 2008;4:387–96.
43. Fu Q, Rahaman MN, Bal BS, Huang W, Day DE. Preparation and bioactive characteristics of a porous 13–93 glass, and fabrication into the articulating surface of a proximal tibia. J Biomed Mater Res Part A. 2007;82A:222–9.
44. Pirhonen E, Moimas L, Haapanen J. Porous bioactive 3-D glass fiber scaffolds for tissue engineering applications manufactured by sintering technique. Key Eng Mater. 2003;240–242:237–40.